POLYMER COLLOIDS

1. Introduction

Polymer colloids are often referred as latexes, and consist of submicrometer polymer particles dispersed in water or organic liquids, which appear as milky fluids. This article deals solely with aqueous dispersions. These dispersions may transform into a polymer film upon drying, which can be clear or opaque, hard or tacky, and plastic or elastic depending on the needs. The polymer film is hardly visible, but provides critical properties in various industrial applications, and also finds ways in academic laboratories as model colloids.

The global production of synthetic polymers has reached ~190 million metric tons with a total value of > U.S.$200 billion in the year 2000. Polymer colloids account for roughly 4% of the synthetic polymer production, corresponding to 7.5 million metric tons of dry polymer or 15 million tons of the polymer colloid, assuming an average polymer content of 50%. This figure is expected to exceed 9 (dry) million metric tons in 2004. One of the most important polymer colloids, natural latex *from Hevea brasiliensis*, amounts to an additional 6 (dry) million metric tons. In some applications (ie, impact modifiers for plastics and cement modifiers), the polymer colloid is further processed as a dry powder by the manufacturers. The above statistics also omit ~1 million tons of these dried polymer colloids produced worldwide (1).

Among these synthetic polymer colloids, styrene–butadiene copolymers, polyacrylates, and vinyl-acetate homopolymers and copolymers account for 95% of the total production, as seen in Fig. 1. Other polymer colloids contain copolymers of ethylene, styrene, vinyl ester, vinyl chloride, vinylidene chloride, chloroprene, and polyurethane.

In excess of 500 companies produce and offer polymer colloids around the world. However, the leading three suppliers—BASF, DOW, and Rohm and Haas—each have an annual production capacity of > 1 (wet) million metric tons, which corresponds to 20% of the world market. Applications such as paints, paper coatings, adhesives, and carpet backing account for nearly 80% of the total production of these synthetic polymer colloids (Fig. 2). Other applications include printing inks, nonwovens, leather finishing, dipping goods, asphalt and concrete modifications, medical applications, and modification of plastic materials.

The earliest patent on the polymer colloid was filed in 1920s, but large industrial-scale production was established only during World War II. This effort by the Government Rubber Styrene (GRS) Project in the United States and Canada (2) was initiated by the shortage of natural rubber in North America. The Canadian rubber plant, built in record time, was producing its first GRS product just slightly > 16 months after the initiation of the project, which included construction of research labs and pilot plants across the United States Canada border. One of the basic polymerization recipes developed through this project is shown in Table 1 (3,4). These recipes are still being used to produce styrene–butadiene–rubber (SBR) latexes for tire productions and other applications, including latex foam, construction adhesives, and asphalt modification.

2. Synthesis of Polymer Colloids

2.1. Emulsion Polymerization. Polymer colloids are produced by the emulsion polymerization process, where an appropriate hydrophobic monomer is dispersed in droplet form in a continuous medium (usually water) through free-radical polymerization as depicted in Fig. 3 (1–3). A simple recipe, which could be used to demonstrate the influence of ingredients and process on polymer and colloidal properties, is shown in Table 2. The water phase contains a sufficient amount of the surfactant [ie, sodium dodecyl sulfate (SDS) in Table 2]. These surfactant molecules are present as free surfactant, aggregated to form micelles above the critical micelle concentration (CMC) and also adsorbed on the surface of monomer droplets. The hydrophobic monomer diffuses through the water and swells the surfactant micelle. The entry of free radicals formed in the water phase (ie, through thermal decomposition of ammonium persulfate) into the monomer-swollen micelles initiates the polymerization, as schematically illustrated in Fig. 3.

The size of these monomer-swollen micelles is typically 5–7 nm in diameter, whereas monomer droplets are at least 1000 $\times$ bigger in diameter. Therefore, the number of monomer-swollen micelles in such a system is orders of magnitude greater than the number of monomer droplets present. Consequently, the ratio of their surface areas is similarly large. For example, a dispersion of 50 wt% monomer droplets in water would contain typically $\sim 10^{10}$ monomer droplets per liter, whereas 10^{17}–10^{19} monomer-swollen micelles would be present. This situation represents a total surface area of the swollen micelles $\sim 10^5$ times that of the monomer droplets. Thus, free radicals produced in the water phase have a far greater probability of entering a micelle and initiating polymerization than entering a monomer droplet. In addition, the overall rate of polymerization, which is the rate per particle multiplied by the number of polymerizing particles, is greatly enhanced in the micellar system. Detailed description of the emulsion polymerization process and the rate of polymerization can be found in Refs. 2, 5–8.

An alternative to micellar nucleation that is widely practiced today in industry is the use of preformed polymer particles of very small and uniform size. In this process, known as seeded emulsion polymerization, these polymer particles act as the nucleus for further polymer growth.

2.2. Manufacturing Processes. All the GRS recipes discussed before, as well as many studies performed in university laboratories up to early 1970s, were developed using a so-called bottle polymerization. Here, degassed or nitrogen saturated water and monomers were charged in a glass bottle with a stopper together with other necessary ingredients and tumbled in a temperature controlled water bath.

Industrial processes are categorized as batch, semibatch, or continuous processes. The processes differ not only in equipment type and economics of operation, but also in the specific properties imparted to the polymer and the dispersion. In a batch emulsion polymerization, all ingredients are added initially to a vessel as in the bottle polymerization, and the monomer/polymer ratio in the

reactor gradually change as the reaction proceeds to completion over a period of time (see Fig. 4**a**).

In a semibatch process, only a portion of the total ingredients is added to the reactor initially, polymerization is initiated and the remainder of the ingredients is added over a period until the desired filling volume is reached. In the semibatch process, conditions in the reactor change rapidly when the feed starts, remain relatively constant for the majority of the feed period, and change rapidly again when the feed stops, as shown in Fig. 4**b**. Fig. 5 shows a modern laboratory facility, which is capable of performing a high pressure emulsion polymerization.

The most common temperature range for emulsion polymerization is 60–100°C using agitated vessels of 15–100 m^3. To control the temperature of these highly exothermic reactions, reactors are fitted with a variety of cooling systems. For safety reasons, semibatch is the preferred manufacturing process with smaller quantities of monomer in the reactor at any given time (1).

The exception is the cold polymerized (below the room temperature) SBR latex utilizing the GRS recipes, where the polymerization is carried out in multiple continuously stirred-tank reactors, CSTR, in series. Here, the reactants continuously enter one of the stirred vessels at the front, and the final product exits from the last reactor in the series. This reaction process is because of the slow polymerization rate at low temperatures to produce the styrene–butadiene polymer with the desired high molecular mass, and low degree of branching and cross-linking. Cross-linking also increases rapidly as conversion increases, necessitating shortstopping of the polymerization at 65–75% conversion when a polymer with high elongation is required (4).

Several works have been published in the literature concerning the controlled radical polymerization process (ie, the living radical polymerization) to achieve better molecular mass and structure control (9,10). The use of nonaqueous systems, such as the supercritical CO_2 has been examined to produce specifically engineered polymers by the emulsion polymerization process (11).

2.3. Major Monomers. The major monomers are those that make up the bulk of the final polymer chains, normally being $> 5\%$ of the final polymer composition. A large number of major monomers are used in emulsion polymerization, either by themselves to give homopolymers or as mixtures giving copolymers (two different monomer units), terpolymers (three different monomer units), or polymers with even higher order.

One of the major determining factors in the choice of a monomer is the glass transition temperature (T_g) of the homopolymer. This is the temperature at which the polymer changes from a glassy state to a plastic or an elastomeric material. This change takes place over a relatively narrow temperature range. Table 3 lists a number of widely used major monomers in order of increasing T_g.

The T_g of polymers made up from mixtures of different monomers can be approximated by use of the Fox equation (12):

$$\frac{1}{T_g} = \frac{W_{m1}}{T_{g1}} + \frac{W_{m2}}{T_{g2}} + \cdots + \frac{W_{mn}}{T_{gn}} \tag{1}$$

where T_g refers to the final polymer, T_{g1}, T_{g2} ... refer to the individual homopolymers, and W_{m1} and W_{m2} ... are the weight fractions of the different monomers

making up the final polymer composition. It can be seen, with *1,3*-butadiene and methylmethacrylate as monomers, that a copolymer can be made with any desired T_g in the range -85°C to $+105^\circ$C. One of the important attributes of polymers that is related to the T_g is the minimum film-forming temperature, MFFT, normally very close to the T_g (13,14). As a polymer colloid dries and the water evaporates, if the polymer is at a higher temperature than the T_g, the molecules in an individual particle have enough freedom of deformation to create a coherent polymer film. Below the T_g, the movement of molecules is too restricted to allow particle deformation, and a coherent film cannot be formed. A comprehensive review on this subject can be found in (15,16).

In addition to its T_g, a given polymer has many other properties of importance. For example, vinyl chloride may be used where fire retardency is required; acrylonitrile can impart solvent resistance; acrylates tend to give good heat and ultraviolet (uv) light stability. The general characteristics that control a polymer's behavior are basic chemical composition, crystallinity, T_g, molecular mass and distribution, gel content, and cross-linking. Some ways in which desired properties can be achieved are shown in Table 4 (1).

2.4. Functional Monomers. Certain monomers containing a functional group such as a carboxylic acid or amide in addition to having the polymerizable C=C double bond are characterized as functional monomers. Those monomers provide special properties to both the polymer and the colloidal properties. They are normally used in relatively small amounts, typically 2–5% of the dry polymer. Acrylic and methacrylic acids are the most widely used monobasic carboxylic acids, while itaconic and fumaric acids are common dibasic acids. These acids, through the C=C bond, participate in the free-radical polymerization in the main polymer chain, but due to the highly polar carboxylic group tend to concentrate at the surface of the polymer particles with the carboxyl group oriented toward the aqueous phase. The dissociated acid groups impart a high degree of mechanical and electrolyte stability to the polymer particles through the electrosteric repulsion.

A scanning microscope photograph of a carboxylated poly(styrene–butadiene) latex film ($T_g = 5^\circ$C) is shown in Fig. 6**a**. Individual polymer particles can be seen even after the polymer colloid transforms to the clear coherent film (17). The carboxylic acid layer covering these polymer surfaces is enhanced with the electron back-scattering image shown in Fig. 6**b**. Here, the carboxylic acid has been stained with uranium-acetate to increase the contrast. The network of the carboxylic acid layers ($T_g > 130^\circ$C) among neighboring particles provides an additional increase in the mechanical strength of the polymer film through ionic cross-linking. The polymer colloid is often used in conjunction with filler particles (ie, clay and calcium carbonate in the paper coating formulation, TiO_2 in the paint, and calcium carbonate in the carpet backing). The functional group on the polymer particles helps dispersing these filler particles in the water phase and provides improved polymer adhesion to the filler surface (18).

3. Colloidal Properties

Typical industrial latex dispersions have 50–60% polymer content, with particles of 100–250 nm in diameter. This means that a 1-L sample of a latex dispersion would contain as many as 4×10^{16} particles with the total surface area of 20,000 m^2, the equivalent of two football fields. In fact, 9 million metric tons of the polymer colloids are expected to be produced in 2004, corresponds to $\sim 5.5 \times 10^{27}$ polymer particles whose total surface area would be equivalent to ~70% of the earth's surface (3.6×10^{14} vs. 5.1×10^{14} m^2, respectively). There is no doubt that this enormous surface area would have a significant influence on their colloidal and application properties. Therefore, it is most appropriate to treat the polymer colloid as a system having three distinct phases: core polymer particles, the surface layer, and the serum phase where the polymer particles are dispersed as schematically illustrated in Fig. 7.

3.1. Particle Size and Size Distribution. Polymer colloids appear milky white, because of their ability to scatter light as small as their particle size. As discussed, the overall rate of polymerization is the rate per particle times the number of polymerizing particles in the reactor; thus, for a given amount of polymer products, the smaller the particles, the faster the overall polymerization rate. The monomer conversion shown in Fig. 4**b** in the semibatch polymerization is highly dependent on the number of particles in the reactor. The rate of polymerization will also influence the bulk polymer properties, such as molecular mass and distribution, branching, cross-linking, etc. Thus, the particle size control is the single most critical parameter for successful emulsion polymerization. The use of a seed eliminates a majority of variability associated with the micellar nucleation.

The dynamic light scattering, DLS (also known as the photon correlation spectroscopy), is routinely employed to estimate the mean particle size of monodisperse polymer colloids. The method measures the Brownian motion of the individual polymer particles dispersed in water, utilizing a highly coherent laser beam. For multimodal and/or polydisperse samples, polymer particles have to be fractionated based on their size. Capillary hydrodynamic fractionation (CHDF), sedimentation field-flow fractionation (SF^3), disk centrifuge, and analytical ultracentrifuge (AUC), techniques have been developed. In addition to the particle size distribution, the AUC can be used to study the chemical composition and molecular mass of the polymer colloid (1).

3.2. Dissociation Behavior of the Surface Layer. The surface layer at the polymer–water interface consists mostly of grafted functional monomers in the recipe. A surface layer consisting of carboxylic groups is compressed at low pH. As the pH in the serum is increased, these acid groups are ionized and the layer expands outward from the particle surface. The dissociation behavior of these acid groups on the latex surface is rather complex, but could be simulated by the Ionizable Surface-Group Model for an ideal system of a molecularly smooth surface covered by a single layer of charge groups (19,20),

$$\mathrm{RCOOH} \leftrightarrow \mathrm{RCOO^-} + \mathrm{H^+} \qquad (2)$$

and

$$K_{\mathrm{a}} = \frac{[\mathrm{RCOO^-}] \cdot a_{\mathrm{s}}(\mathrm{H^+})}{[\mathrm{RCOOH}]} \tag{3}$$

where K_{a} is the dissociation constant for the surface group and $a_s(\mathrm{H^+})$ is the activity of hydrogen ions in the vicinity of the $\mathrm{COO^-}$ site on the surface. By assuming $a_s(\mathrm{H^+})$ is related to the bulk hydrogen-ion activity $a_{\mathrm{b}}(\mathrm{H^+})$ by

$$a_s(\mathrm{H^+}) = a_b(\mathrm{H^+}) \exp(-y_0) \tag{4}$$

where y_0 is the reduced surface potential:

$$y_0 = \frac{\mathrm{e}\psi_{\mathrm{b}}}{kT} \tag{5}$$

where e is the electron charge, ψ_0 is the surface potential, k is the Boltzmann constant, and T is the absolute temperature. $a_s(\mathrm{H^+}) > a_b(\mathrm{H^+})$ since $\exp(-\mathrm{y_0}) > 1$ because of $\psi_0 < 0$ for the negatively charged surface. Thus equation 4 implies that hydrogen ions are preferentially accumulated near the negatively charged latex surface. Equation 4 may be rewritten as

$$\mathrm{pH}_s = -\log\{a_s(\mathrm{H^+})\} = \mathrm{pH}_b + \frac{y_0}{2.303} \tag{6}$$

Equation 6 indicates that $\mathrm{pH}_s < \mathrm{pH_b}$ since $y_{\mathrm{o}} < 0$, where pH_s and pH_b are the *pH* in the vicinity of the surface and in the bulk solution, respectively. This derivation assumes that these effects are solely due to the Coulombic interaction between the positive hydrogen ions and the negatively charged surface.

If we assume that the surface charge of the latex is due to the dissociation of the carboxyl group, the surface charge density, σ_0, is given simply by

$$\sigma_0 - \mathrm{e}[\mathrm{COO^-}] \tag{7}$$

The total surface density of functional groups, N_s, is given by

$$N_s = [\mathrm{COO^-}] + [\mathrm{COOH}] \tag{8}$$

Combining the above equations results in

$$\sigma_0 = \frac{-\mathrm{e}N_s}{1 + [a_b(\mathrm{H^+})/K_a] \exp(-y_0)} \tag{9}$$

The calculated relationship between the fraction of carboxyl groups dissociated, $-\sigma_0/\mathrm{e}Ns$, as a function of pH_b in aqueous NaCl solutions of 10^{-4}, 10^{-3}, 10^{-2}, and $10^{-1}M$ is shown in Fig. 8**a** and 8**b** (19). The values of $N_s = 2 \times 10^{17}$ and 2×10^{18} $\mathrm{m^{-2}}$ (5 and 0.5 $\mathrm{nm^2}$/site, respectively) at $\mathrm{p}K_a = 4.5$ correspond to 1/10 and full monolayer coverage of carboxyl groups on the latex surface (polymer–water interface).

The figures demonstrate that the dissociation behavior of charged groups on the surface is complex and depends strongly on the value of N_s and on the electrolyte concentration in the serum. Industrial polymer colloids typically contain 10^{-2}–$10^{-1}M$ monovalent cations in the serum, and multilayer coverages of the carboxyl groups. In such a system, $pH_b > 9$ would be needed to dissociate 90% of the carboxylic acids on the surface. In a real polymer colloid, the surface layer has a finite thickness. The dissociation of the outermost carboxylic acid in the surface layer will significantly retard the dissociation of the same groups present in the vicinity of the polymer core. Thus, determining the surface charge density from conductometric and potentiometric titration data is nontrivial.

3.3. Electrokinetic Measurements. Electrophoresis is one of the most commonly used experimental techniques for characterizing polymer colloids. In this technique, the velocity of charged particles moving under the influence of the applied electric field is determined. The recent development of the laser Doppler apparatus makes the measurement easy to perform. However, correlating the measured electrophoretic mobility to the surface charge density is, again, a difficult matter. The electrophoretic mobility is not directly related to the surface potential but rather to the ζ-potential, which is the potential somewhere in the surface layer surrounding the polymer particle. Its exact location (often defined as the shear plane) is unknown. The value of ζ is highly dependent on the thickness and nature of the surface layer, and the ionic strength, which is the product of the electrolyte concentration and the counterion valency squared. However, ζ is only weakly related to the surface potential (thus the surface charge density) (20,21). For an ideal particle having a monolayer of carboxylic acids on a molecularly smooth surface (ie, carboxylated polystyrene latex after heat treatment), the ζ-potential is the potential at 0.6 nm from the particle surface, which is just outside of the dissociated carboxylic acid groups (20,22).

The shear plane also moves outward when the surface layer extends toward the bulk water due to the ionization of charged groups. In some cases, this would even cause a reduction in the ζ-potential; a reduced ζ-potential with increasing charge density of the surface layer! This happens most often for small particles at low electrolyte concentration (ie, < 200 nm and $< 10^{-3}$ M monovalent electrolyte), a typical condition for the electrokinetic measurement of most polymer colloids.

The presence of nonionic functional groups (eg, acrylamides) promotes the expansion of the surface layer without increasing its charge density, thus further reducing the ζ-potential. This phenomenon can be used to monitor the grafting reaction of the acrylamide on the carboxylated poly(styrene–butadiene) latex surface during polymerization, as shown in Fig. 9. Here, a small amount of the latex sample was withdrawn from the reactor and its ζ-potential determined in 3×10^{-2} M NaCl at pH 8.0. The measured ζ-potential maintains its high negative value of Ca. -70 mV throughout the polymerization, then suddenly drops to -25 mV at $> 95\%$ monomer conversion. This result demonstrates that the grafting reaction of acrylamide occurs only at the end of the polymerization.

3.4. Rheological Properties. The expanded surface layers consist mostly of water, but they have a significant contribution to the hydrodynamic diameter of the polymer particles, and thus increase the dispersion viscosity as

the pH is increased. The smaller the polymer particles, the larger the contribution of the surface layer to the fractional increase in the hydrodynamic volume.

The viscosity of the polymer colloid can be understood through the aid of the equation proposed by van de Ven (23):

$$\mu = \mu_0 \left[\frac{1 - C/C_m}{1 - (k_0 C_m - 1)C/C_m} \right]^{\frac{-2.5C_m}{2 - k_0 C_m}} \tag{10}$$

where μ_0 is the serum viscosity, C is the hydrodynamic volume fraction that includes contributions due to the surface layer, C_m is the hydrodynamic volume fraction at the maximum packing, and k_0 represents the degree of particle–particle interactions. The parameter C_m and k_0 are ~ 0.65 and 2.0, respectively, for a dispersion with a narrow particle size distribution at a high enough shear rate (ie, $>100\ s^{-1}$).

Fig. 10**a** and 10**b** illustrate the change in the dispersion viscosity as a function of the volume fraction of the polymer for monodispersed particles of 140 and 200 nm in diameter, respectively. The serum viscosity of these dispersions was assumed to be 2 mPa·s, since a typical polymer colloid contains a small amount of water-soluble materials. When the surface layer is completely collapsed (ie, carboxylic groups at low pH), both dispersions have an identical viscosity versus polymer solids relationship; gradually increasing its viscosity from 48 to near 500 mPa · s, as the polymer solids increase from 48 to 56%.

Because the expanded surface layer consists mostly of water, it does not contribute to the polymer volume fraction estimated from the dry weight. However, it can have significant contribution to the hydrodynamic volume fraction of the dispersion, especially for a polymer colloid with small particles. This fact causes a sharp increase in the dispersion viscosity for polymer particles with an extended surface layer. The viscosity of a polymer colloid with 140 nm particles will exceed 10,000 mPa · solids if the surface layer extends to 5 nm from the core particle surface. If the same surface layer covers 200 nm particles, the viscosity would only be slightly $>$ 400 mPa·s, a difference of $> 250\times$ in the viscosity at the same solid content, as seen in Fig. **a** and **b**.

It is often desirable to achieve the highest possible polymer content, while maintaining a low enough viscosity (ie, $<$ 2 Pa·s) for ease of handling. This condition can be achieved by having either a bimodal or broad particle size distribution (24,25). An example of this can be found in the SBR latex developed during and after the GRS project. As discussed, the cold polymerization is employed to achieve the desired high molecular mass, as well as low branching and cross-link formation. To achieve the adequate polymerization rate (which is the rate per particle multiplied by the number of polymerizing particles), the particle size is controlled to be 70–90 nm in diameter. Either freezing or a high pressure process is employed to agglomerate these primary particles to produce polymer colloids with a broad size distribution ranging from 70 nm to a few micrometer in diameter. The resultant high solids dispersion of $\sim$70% polymer content, after the water content has been reduced by low-pressure evaporation, has a viscosity $<$ 2Pa·s ($C_m > 0.8$ in eq. 10). Without the agglomeration process, the dispersion

would have the same viscosity at a polymer contents $< 50\%$. A number of processes producing bimodal or broad particle size have been developed.

3.5. Serum Composition. A small increase in the serum viscosity (μ_0 in eq. 10) would have significant influence on the viscosity of the concentrated dispersion; 350–700 mPa·s values by just doubling the serum viscosity from 2–4mPa·s. A small amount of a thickener is added to the latex dispersion to have the desired rheological properties; ie, a high low shear, but low high shear viscosity. Discussions on the use of associative thickeners, their interactions with latex particles and resulting effects on the dispersion stability can be found in Ref. (26).

The surfactant is one of the critical ingredients in the serum to produce the micelles, where the polymerization initiates, and the adsorbed surfactant molecules provide dispersion stability of the growing particles through electrostatic interaction. Additional surfactants are often added after the polymerization to have desired properties for specific applications. These include nonionic surfactants in paper-coating latexes to improve the high shear stability of their coating formulation and anionic surfactants to improve foaming characteristics of carpet-backing compounds.

Foaming could be detrimental to the paints and paper-coating process, and may necessitate the addition of an adequate defoamer. A water-soluble plasticizer would be needed to promote film forming of a high T_g polymer for the paint application. Rosin acid derivatives are often added as a tackifier for some of adhesive latex formulations. As discussed, the mechanical strength of the polymer film is increased by the carboxylic group on the polymer particle surface, and in fact can be increased further by the use of, eg, zinc oxide added in the serum, which gives an ionic cross link among these surface groups. The presence of the carboxylic groups also allows cross linking with urea–formaldehyde, phenol–formaldehyde, melamine–formaldehyde, and various epoxy resins post-added to the serum.

4. Polymer Morphology

One particle of a polymer colloid could contain a few to tens of thousands of macromolecules, each of which consists of hundreds to millions of monomer units. They may be homopolymers, copolymers, terpolymers, or polymers with even higher order. Some applications require contradictory polymer properties; ie, a soft polymer property for low film forming temperature, but a hard polymer property for the maximum block resistance of the painted surface. This requirement can be achieved with polymer colloids having a heterogeneous particle morphology, as illustrated in Fig. 11 (1,27,28). These structures can be created through the sequential addition of two distinct monomers, and result due to the difference in the thermodynamic and kinetic properties of the resulting polymer–monomer phases during emulsion polymerization.

The thermodynamic principle governing the formation of these heterogeneous particle morphologies was demonstrated by the pioneering work of Torza and Mason (29), who investigated coalescence of two immiscible liquid drops, phase 1 and phase 3 suspended in a third immiscible liquid, phase 2.

When two drops are brought into contact, three equilibrium configurations, which depend on three interfacial tensions γ_{ij} ($i \neq j \neq k = 1,2,3$), are possible as illustrated in Fig. 12. By convention, phase 1 is designated as the phase for which $\gamma_{12} > \gamma_{23}$. When $\gamma_{12} > \gamma_{23} + \gamma_{13}$, the phase 1 will be entirely engulfed by phase 3 to form a spherical drop, which has two spherical interfaces (2–3 and 1–3). For the nonengulfing condition of $\gamma_{13} > \gamma_{12} + \gamma_{23}$, the interface between phase 1 and 3 cannot form spontaneously, and the drops remain separated. The interfacial tensions and initial radii of the drops determine the geometrical details of the resulting drop of the partial engulfing system, as shown in the middle of Fig. 12.

Hollow latex particles have specific interest in paper coating and paints for their excellent gloss development and light scattering capabilities with reduced weight. Numerous emulsion polymerization processes have been developed to produce these unique polymer particle structures. A comprehensive review on the synthesis and applications of hollow latex particles can be found in (30).

5. Model Colloids

A dispersion consisting of spherical particles of almost equal size can be an ideal model colloid for light scattering, dispersion stability (31), drying, and the film-formation processes (32), for rheological studies, etc. A concentrated dispersion of the monodisperse latex particles (or a dilute dispersion with a clean serum) develops iridescent color, caused by Bragg diffraction from the crystalline superstructure of closely packed particles (33–35). In addition to satisfying academic curiosity, these close-packed monodisperse polymer particles have been used successfully to construct filtering media having almost identical pore sizes (36), and currently being investigated to construct a new generation of information storage and printing media, as shown in Fig. 13 (37).

BIBLIOGRAPHY

CITED PUBLICATIONS

1. D. Urban and K. Takamura, ed., *Polymer colloids and Their Industrial Applications*, Wiley-VCH, 2002.
2. D. C. Blackley, *Emulsion Polymerization Theory and Practice*, Applied Science Publishers Ltd., London, 1975.
3. B. C. Proyor, E. W. Harrington, and D. Druesedow, *Ind. Eng. Chem.* **45**, 1311 (1953).
4. L. H. Howland, V. C. Neklutin, R. L. Provost, and F. A. Mauger, *Ind. Eng. Chem.* **45**, 1304, (1953).
5. W. D. Harkins, *J. Am. Chem. Soc.* **69**, 1428, (1947); *J. Polymer Sci.* **5**, 217 (1950).
6. W. V. Smith and R. H. Eward, *J. Chem. Phys.* **16**, 592 (1948).
7. J. Ugelstad and F. K. Hansen, *Rubber Chem. Technol.* **49**, 536 (1976).
8. I. Capek, *Adv. Colloid Inteface Sci.* **99**, 77 (2002).

9. J. Qiu, B. Charleux, and K. Matyjaszewski, *Prog. Polym. Sci.* **26**, 2083 (2001).
10. F. D'Agosto, M. Charreyre, C. Richot, and R. G. Gilbert, *J. Poly. Sci.* **41**, 1188 (2003).
11. J. L. Young and J. M. DeSimone, *Pure Appl. Chem.* **72**, 1357 (2000).
12. T. G. Fox and P. J. Flory, *J. Appl. Phys.* **21**, 581 (1950).
13. A. F. Routh, W. B. Russel, J. Tang, and M. S. El-Aasser, *J. Coat. Tech.* **73**, 41 (2001).
14. M. Visschers, J. Laven, and R. V. D. Linde, *J. Coat. Tech.* **73**, 49 (2001).
15. P. A. Steward, J. Hearn, and M. C. Wilkinson, *Adv. Colloid Interface Sci.* **86**, 195 (2000).
16. J. L. Keddie, *Mater. Sci. Eng.* **R21**(3), 101 (1997).
17. Y. Ming, K. Takamura, H. T. Davis, and L. E. Scriven, *TAPPI J.* **78**(11), 151 (1995).
18. J. G. Sheehan, K. Takamura, H. T. Davis, and L. E. Scriven, *TAPPI J.* **76**(12), 93 (1993).
19. K. Takamura and R. S. Chow, *Colloids Surfaces* **15**, 35 (1985).
20. R. S. Chow and K. Takamura, *J. Colloid Inter. Sci.* **125**, 226 (1988).
21. R. J. Hunter, Zeta *Potential in Colloid Science, Principles and applications*, Academic Press, New York, 1981.
22. R. S. Chow, and K. Takamura, *J. Colloid Inter. Sci.* **125**, 212 (1988).
23. T. G. M. van de Ven, *Colloidal Hydrodynamics*, Academic Press, New York, 1989, p. 541.
24. R. D. Sudduth, *J. Appl. Polym. Sci.* **66**, 2319 (1997).
25. R. D. Sudduth, *J. Coating Tech.* **75**, 35 (2003).
26. E. Kostansek, *J. Coating Tech.* **75**, 27 (2003).
27. D. Sundberg and co-workers, *J. Appl. Polym. Sci.* **41**, 1425 (1990).
28. L. E. Karlsson, O. J. Karlsson, and D. C. Sundberg, *J. Appl. Polym. Sci.* **90**, 905 (2003).
29. S. Torza, and S. G. Mason, *Science* **163**, 813 (1969).
30. C. J. McDonald, and M. J. Devon, *Adv. Colloid Polymer Sci.* **99**, 181 (2002).
31. K. Takamura, H. L. Goldsmith, and S. G. Mason, *J. Colloid Inter. Sci.* **82**, 175 (1981).
32. J. M. Salamanca and co-workers, *Langmuir* **17**, 3202 (2001).
33. R. M. Fitch, ed., *Polymer Colloids: A Comprehensive Introduction*, Academic Press, New York, 1997.
34. T. Okubo, H. Kimura, T. Kawai, and H. Niimi, *Langmuir* **19**, 6014 (2003).
35. K. Wormuth, M. Herzhoff, and O. Brüggemann, *Colloid Polym. Sci.* **280**, 432 (2002).
36. S. Jons, P. Ries, and C. J. McDonald, *J. Membrane Sci.* **155**, 79 (1999), C. J. McDonald, R. K. Prud'homme, and J. D. Carbeck, *J. Membrane Sci.* **231**, 57 (2004).
37. H. Fudouzi, and Y. Xia, *Langmuir* **19**, 9653 (2003).

KOICHI TAKAMURA
BASF Corporation Charlotte Technical Center

Table 1. **The Basic Recipe for the Initial Plant Production of SFS Based GRS 1500**[a]

Ingredients	Amounts
butadiene	71
styrene	29
water	200
PMHP[b]	0.08
SFS[c]	0.08
$FeSO_4$ $7H_2O$	0.03
EDTA	0.035
Dresinate 214[d]	4.5
Na_3PO_4 $12H_2O$	0.5
Sulfole B-8[e]	as required

[a]From Ref. 4.
[b]*p*-Menthane hydroperoxide.
[c]Sodium formaldehyde sulfoxylate.
[d]Oleic acid.
[e]*tert*-Dodecyl mercaptan.

Table 2. **Model System for the Study of Some Aspects of Emulsion Polymerization**[a]

Ingredient	Quantity (phm)[b]	Influence
water	100–150	solid content, viscosity, heat transfer
styrene	0–95	T_g, minimum film forming temperature
n-butyl acrylate	0–95	T_g, minimum film forming temperature
methacrylic acid	0–5	colloidal stablity, viscosity, reaction kinetics
sodium dodecyl sulfate	0.5–3.0	particle size, colloidal stability, reaction kinetics
ammonium persulfate	0.1–1.0	particle size, reaction kinetics, molecular mass
tert-dodecyl mercaptan	0–1.0	molecular mass, reaction kinetics
divinylbenzene	0–0.5	cross-linking/gel formation

[a]From Ref. 1, p.m.
[b]Parts per 100 parts of monomer.

Table 3. **Some Major Polymers Used in Emulsion Polymerization**

Monomer	T_g of Homopolymer °C
1,3-butadiene	−85
n-butyl acrylate	−54
2-ethylhexyl acrylate	−50
methyl acrylate	10
vinyl acetate	32
vinyl chloride	81
acrylonitrile	98
styrene	100
methyl methacrylate	105

Table 4. **Some Aspects of Polymer Design through Composition**[a]

Desired property	Possible polymer design
stiffness	use methacrylates, acrylonitrile, styrene
soft hand	use *n*-butyl acrylate, ethyl acrylate, butadiene
tackiness	use 2-ethylhexyl or hexyl acrylate
water resistance	use cross-linking monomers; *N*-methylol(meth)acrylamide use hydrophobic monomers; *n*-butyl acrylate or styrene
resistance to organic solvents	cross-linking monomers and/or acrylonitrile
high tensile strength	high T_g monomers; styrene, acrylonitrile, or methyl methacrylate
high elongation	low T_g monomers; *n*-butyl acrylate, or butadiene
thermoformability	avoid cross-linking. Use thermoplastic monomers; styrene
high alkali swellability	use high amounts of polymerizable acids: acrylic acid

[a]From Ref. 1, p. 25.

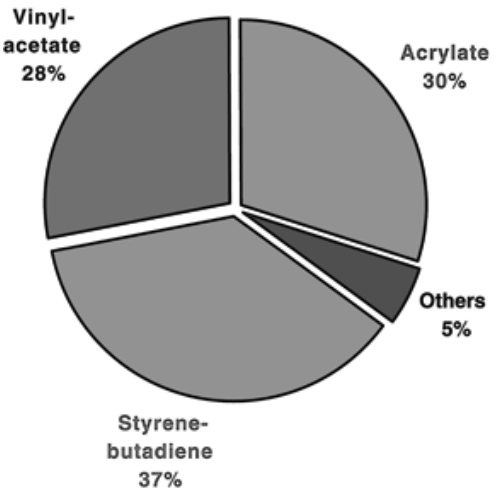

Fig. 1. Three major polymer types account for 95% of the total polymer colloids (from Ref. 1, p. 12).

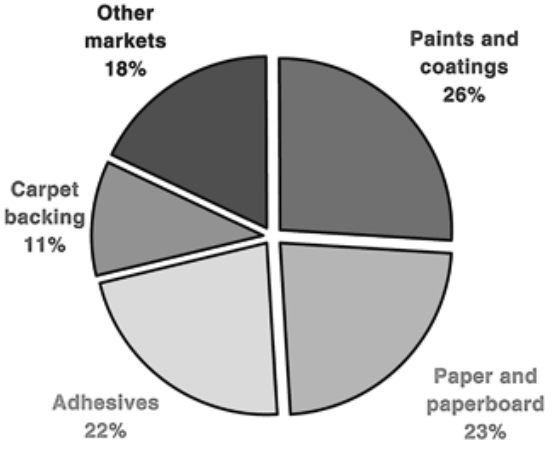

Fig. 2. Major applications of the polymer colloid in global market (from Ref. 1, p. 75).

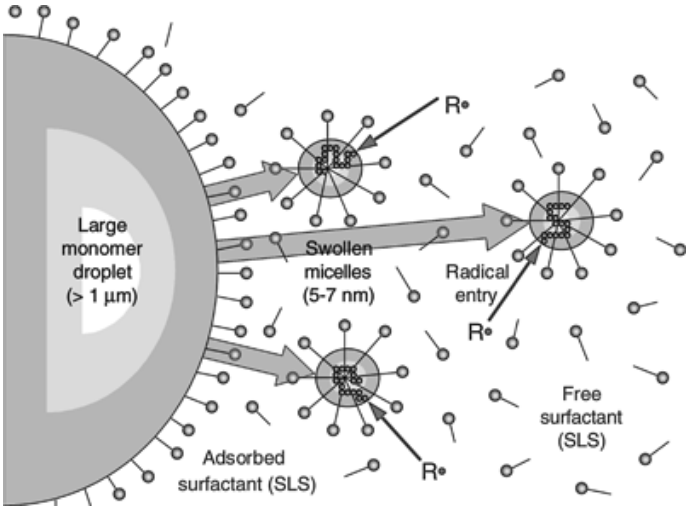

Fig. 3. Schematic illustration of the emulsion polymerization. The schematic diagram is a courtesy of C. D. Anderson, and M. S. El-Aasser, Emulsion Polymerization Institute, Lehigh University, Bethlehem, Penn.

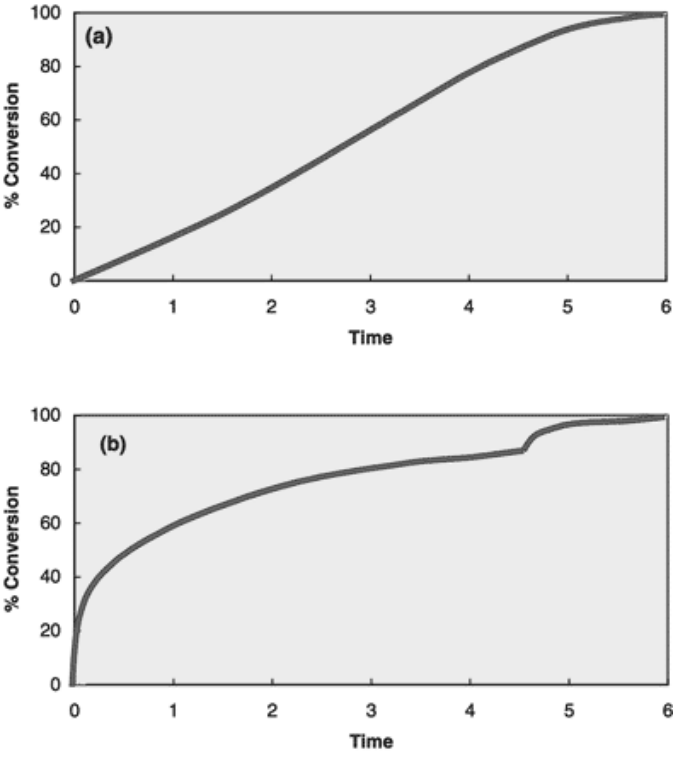

Fig. 4. Variation in monomer/polymer ratio in (**a**) batch and (**b**) semibatch processes.

Fig. 5. Laboratory equipment for emulsion polymerization at high pressures. (Photograph courtesy of BASF Corporation.)

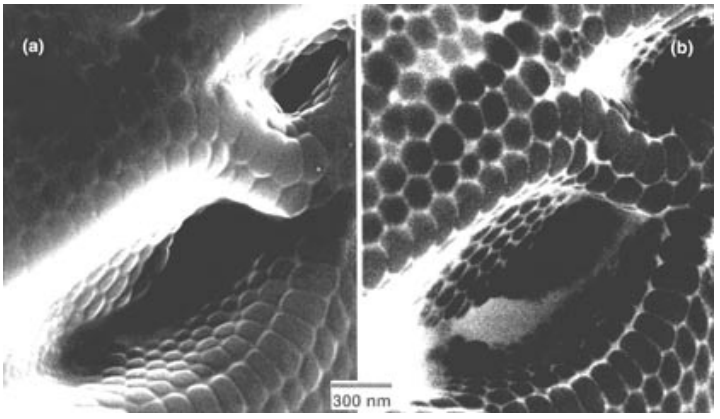

Fig. 6. (**a**). Field emission scanning electron microscope photographs of the carboxylated poly(styrene–butadiene) latex film. (**b**). Back scattered electron image showing carboxylic acid layer covering individual particles (from Ref. 18).

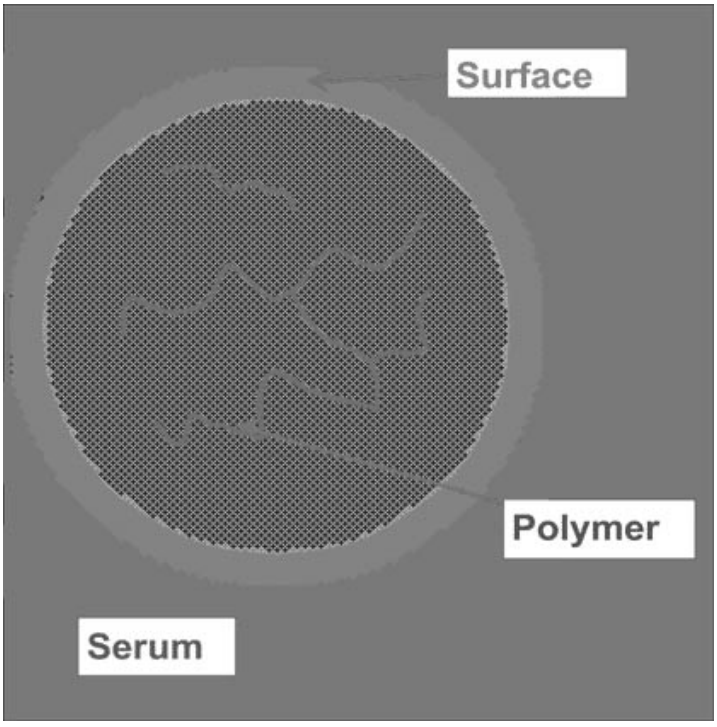

Fig. 7. Schematic diagram for polymer colloid showing core polymer particle, surface layer, and serum.

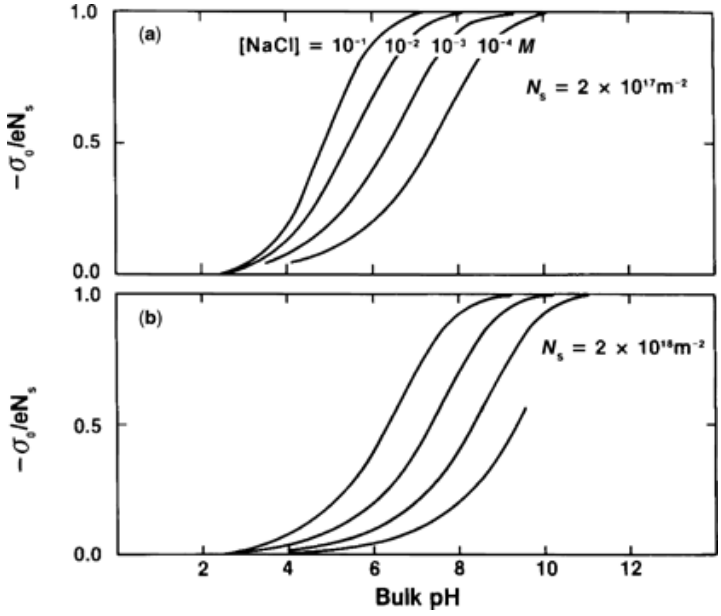

Fig. 8. Calculated fraction of dissociated surface groups, $-\sigma_0/eN_s$, as a function of bulk pH in aqueous NaCl solutions of 10^{-4}, 10^{-3},10^{-2}, and 10^{-1} M at 30°C. (**a**) $N_s = 2 \times 10^{17} m^{-2}$ (5 nm^2/site) and (**b**) $N_s = 2 \times 10^{18}$ m^{-2} (0.5 nm^2/site) (from Ref. 20).

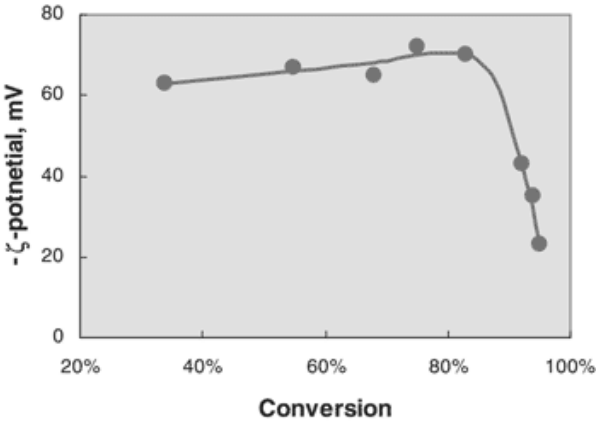

Fig. 9. Monitoring grafting reaction of acrylamide on carboxylated latex surface through change in measured ζ-potential measured in 3×10^{-2} M NaCl at pH = 8.0.

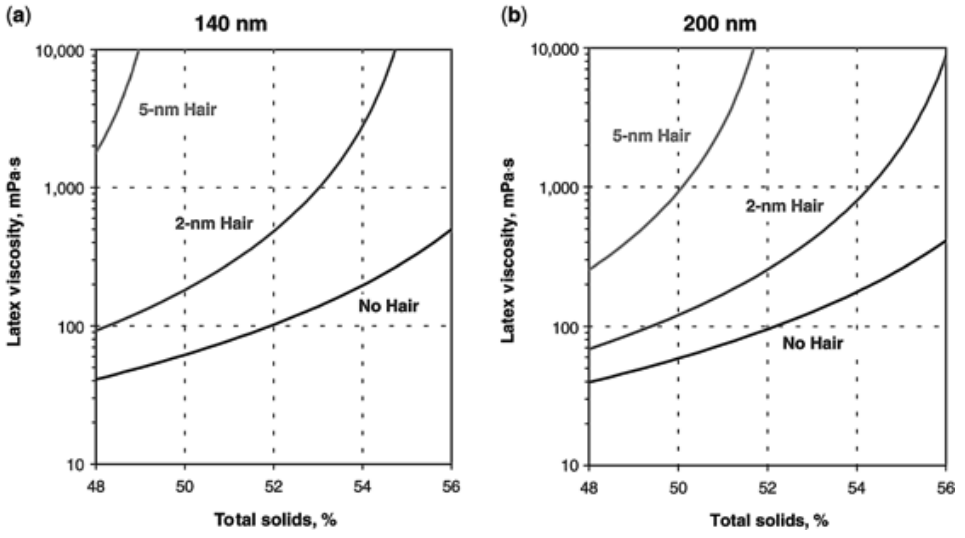

Fig. 10. Estimated viscosity of a polymer colloid as a function of polymer solids (assuming density = 1.0) with various thickness of the surface layer for particles of (**a**) 140 nm and (**b**) 200 nm in diameter.

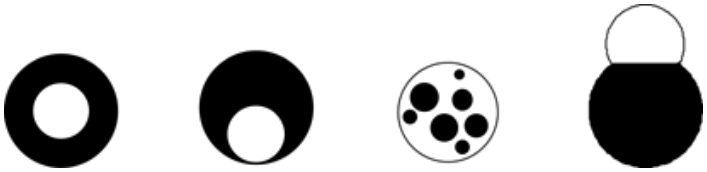

Fig. 11. Schematic illustration showing examples of particle morphologies (from Ref. 1, p. 70).

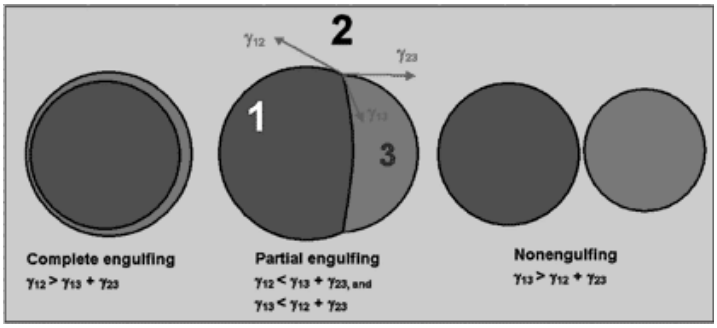

Fig. 12. Three equilibrium configurations of two immiscible liquid drops suspended in a third immiscible liquid (30). The phase 1 is designated as that phase for which γ_{12}, the interfacial tension between phase 1 and 2, is $> \gamma_{23}$.

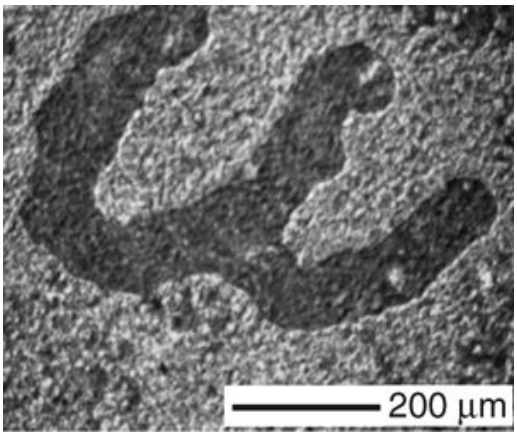

Fig. 13. Reflective optical micrograph of a Greek character generated by microcontact printing on a rigid photonic paper, which is a colloidal crystal of polymer particles embedded in an elastomer matrix made of poly(dimethylsiloxane) (see Ref. 37 for details).